Materials Transactions, Vol. 43, No. 8 (2002) pp. 1931 to 1936
Special Issue on Bulk Amorphous, Nano-Crystalline and Nano-Quasicrystalline Alloys IV

Electrical Resistivity and Mössbauer Studies for the Structural Relaxation Process in Pd–Cu–Ni–P Glasses

Osami Haruyama[1], Hisamichi M. Kimura[2], Nobuyuki Nishiyama[3], Akihisa Inoue[2] and Juichiro Arai[1]

[1]*Department of Physics, Faculty of Science and Technology, Tokyo University of Science, Noda 278-8510, Japan*
[2]*Institute for Materials Research, Tohoku University, Sendai 980-8577, Japan*
[3]*Inoue Supercooled Glass Project, ERATO, Japan Science and Technology Corporation, Sendai 980-0807, Japan*

The structural relaxation process in several Pd–Cu–Ni–P glasses was investigated by the electrical resistivity and the Mössbauer experiments. The change in the resistivity, $\rho(300)$, and the corresponding slope, $\alpha(300) = (\mathrm{d}\rho/\mathrm{d}T)_{300}$, at room temperature was measured after a given heat treatment. The change in $\rho(300)$ with isochronal annealing below the glass transition temperature (≈ 572 K), starting from room temperature, demonstrated that the $\rho(300)$ increased with temperature and decreased beyond 550 K. The isothermal annealing at 570 K exhibited that the $\rho(300)$ showed an increase, about 1%, during an initial annealing stage for 3.0×10^2 s and remained almost constant up to 6.0×10^3 s, and hereafter monotonously decreased. The change in $\alpha(300)$ showed an opposite sign to that in $\rho(300)$. The reversible change in $\rho(300)$ due to isochronal annealing was observed in the heat treatment repeated between 350 and 550 K. The Mössbauer spectroscopy experiments were performed at room temperature to investigate the local structure change due to structural relaxation. The isomer shift and the quadrupole splitting for an annealed sample decreased in comparison with that of an as-quenched sample. Based on these results, the structural relaxation process and the structure change were discussed within the framework of the free volume model.

(Received March 13, 2002; Accepted May 22, 2002)

Keywords: *structural relaxation, electrical resistivity, weak localization, Mössbauer spectroscopy, free volume model*

1. Introduction

Since Pd–Cu–Ni–P glasses posses a wide supercooled liquid region ($\Delta T_x = T_x - T_g \approx 95$ K[1)]), a high resistance to crystallization[1)] and a small critical cooling rate (0.067 K/s[2)]), they are very interesting objects from a scientific point of view and have a great potential for the industrial use. Some curious reports have been presented on local atomic structure,[3)] thermal property,[1,2)] viscous flow behavior,[4)] specific heat,[5)] electrical resistivity[6)] and so on. It is widely recognized that the structural relaxation has a great influence on physical properties of metallic glasses. However, there are few studies on the structural relaxation behavior of these Pd–Cu–Ni–P glasses. Following the free volume model,[7)] the structure relaxation is the process that the free volume content approaches to an equilibrium value by the annihilation of a quenched-in excess free volume. Since the atomic configuration is varied by a collective motion of atom groups, this process is called the topological short range ordering (TSRO) process.[8)] Also, there exits another relaxation process, suggesting that a compositional fluctuation in the sample becomes larger. This process is called the chemical short range ordering (CSRO) process.[8)] In a thoroughly stabilized glass, possessing approximately an equilibrium free volume concentration, the CSRO process is possible to separate from the TSRO process.[9,10)] The local change in amorphous structure due to the structural relaxation has been investigated by diffractive methods.[11,12)] In concerning with TSRO process for the Pd–Ni–Si glass, authors pointed out that a tendency to phase separation appeared after annealing just below glass transition,[13)] together with a effect of the free volume annihilation. However, this should not be applicable to the metallic glass in general. The common structural model about the CSRO process is not established so far. Srolovitz *et al.*[14)] has previously presented a model on the structural relaxation, obtained by the analysis of the stress distribution in the amorphous structure. They pointed out that the TSRO process corresponded to the relaxation of the hydrostatic inner stress and the CSRO process was connected with a redistribution of the shear stress component. Brüning *et al.*[15)] has examined the structural relaxation process in the $Pd_{40}Ni_{40}P_{20}$ glass. They confirmed that the structure factor $S(Q)$ changed according to Srolovitz's considerations. In addition, they examined the local structure change due to the structural relaxation by Mössbauer spectroscopy. They concluded that TSRO and CSRO processes involved an essentially identical microscopic change, relating to the motion and rearrangement of metal atoms.

In the present study, we examine the TSRO behavior at relatively high temperatures just below glass transition, mainly, by means of the electrical resistivity measurement. We also perform Mössbauer spectroscopy for 1 at% ^{57}Fe doped $Pd_{40}Cu_{30}Ni_9Fe_1P_{20}$ glass to investigate the structural change due to the structural relaxation, mainly connected with the TSRO process. It was reported that the volume change via relaxation was approximately 0.5%[16)] for the $Pd_{40}Cu_{30}Ni_{10}P_{20}$ glass. This is comparable with a volume change, 0.13–0.51%, reported as due to the structural relaxation in metallic glasses.[17)] Thus, it is predicted that the CSRO process extends similarly in Pd–Cu–Ni–P glasses through the rearrangement of atoms due to the TSRO process. We examine whether or not there exists the CSRO process in the present glasses and, if possible, the kinetics of the CSRO process using the relaxation function.

2. Experimental Procedure

The master alloy with the composition of $Pd_{40}Cu_{30}Ni_{30}P_{20}$ was prepared by arc melting using the mixture of elements, 99.99%Pd, 99.99%Cu, 99.99%Ni and the $Pd_{60}P_{40}$ alloy, synthesized by sintering as reported previously.[1)] The 1 at% ^{57}Fe-

doped $Pd_{40}Cu_{30}Ni_9Fe_1P_{20}$ master alloy for Mössbauer measurement was similarly prepared. The $Pd_{42.5}Cu_{27.5}Ni_{10}P_{20}$ ingot was prepared by sintering the mixture of each metal element and 99.9995%P (the granular red phosphorous) in an evacuated quartz tube and holding it at 1370 K for 24 h, and then cooling it to room temperature. For the $Pd_{40}Cu_{30}Ni_{30}P_{20}$ and the $Pd_{40}Cu_{30}Ni_9Fe_1P_{20}$ alloys, the B_2O_3 flux (99.999%) treatment was made in preparing them by arc melting. The $Pd_{42.5}Cu_{27.5}Ni_{10}P_{20}$ alloy was flux-treated by holding it at 1300 K for 6 days in an evacuated quartz tube. Glass ribbons, having cross sections of approximately $1.5 \times 0.04\,mm^2$ for quaternary glasses and $5.0 \times 0.05\,mm^2$ for Fe-doped glass, were prepared by conventional melt-spinning method with the peripheral velocity, approximately 20 m/s, of a copper wheel in an Ar gas atmosphere. The amorphous nature of samples was checked by X-ray diffraction using Cu–Kα radiation and differential scanning calorimetry (DSC), operated at a heating rate of 0.67 K/s. The electrical resistivity measurement was performed by usual d.c four probes technique. The residual resistivity, $\rho(300)$, at room temperature and the corresponding slope, $(d\rho/dT)_{300}$, were estimated by a least square fit to the resistivity data measured between 293 and 343 K after a given heat treatment. The d.c current was supplied by a Rigaku R6161 source meter and it was so stable that the fluctuation was negligible during the experiment. The Keithley 182 nano-volt meter, having a precision within ± 50 nV, was used to measure the voltage change. The density of the bulk $Pd_{40}Cu_{30}Ni_{10}P_{20}$ glass, prepared by water quenching, was measured at room temperature by Archimedes' principle with a toluene as a working fluid.

The Mössbauer experiments were performed in conventional transmission geometry at room temperature using a ^{57}Co (Rh) source driven in constant-acceleration mode. All isomer shifts were calibrated with respective to the center of α-Fe spectrum.

3. Results

Figure 1 shows the electrical resistivity, $\rho(T)/\rho(300)$, as a function of annealing temperature for the $Pd_{40}Cu_{30}Ni_{10}P_{20}$, the $Pd_{42.5}Cu_{27.5}Ni_{10}P_{20}$ and the $Pd_{40}Cu_{30}Ni_9Fe_1P_{20}$ glasses. These glasses all show a negative TCR (temperature coefficient of resistivity) at room temperature and the resistivity decreases with increasing temperature. The glass transition temperature, T_g, and the crystallization temperature, T_x, are defined from DSC curves, and are summarized in Table 1. The influence of Fe-doping on the thermodynamic properties is not significant, because both of T_g and T_x were almost unchanged for the $Pd_{40}Cu_{30}Ni_9Fe_1P_{20}$ glass in comparison with those of the $Pd_{40}Cu_{30}Ni_{10}P_{20}$ glass. The resistivity behavior in the supercooled liquid region seems to be complicated for the $Pd_{42.5}Cu_{27.5}Ni_{10}P_{20}$ glass, but it may be apparent and not essential. Nishiyama *et al.* reported[4] that the viscosity of the $Pd_{40}Cu_{30}Ni_{10}P_{20}$ glass became significantly small in the supercooled liquid region. Thus, the shape of the sample may be changed due to the surface tension of the sample in a supercooled liquid state. Authors performed the resistivity measurement using a bulk $Pd_{40}Cu_{30}Ni_{10}P_{20}$ glass[6] and confirmed the validity of this consideration. In fact, then, the resistivity decreased steadily with increasing temperature after entering the supercooled liquid region. To examine the influence of the temperature on the evolution of the structural relaxation, the room temperature resistivity, $\rho(300)$, and the slope, $\alpha(300) = (d\rho/dT)_{300}$, were measured after annealing an as-quenched $Pd_{42.5}Cu_{27.5}Ni_{10}P_{20}$ glass ribbon isochronally for 1.2×10^3 s at each temperature. The experiment started at room temperature. The results are shown in Fig. 2. Two kinetic phenomena, relating to the free volume and the chemical order, compete with each other during the isochronal treatment between room temperature and glass transition temperature. The increase of $\rho(300)/\rho_{as}(300)$ demonstrates that while the quenched-in stress is released with annealing, the chemical order is newly formed, because it remains at a low level in an as-quenched glass,[10,18] and the quenched-in free volume is eliminated in direction to an equilibrium concentration. Above 560 K, the resistance starts to decrease. This is interpreted in such a way that (1) the chemical order is decomposed, because the magnitude of equilibrium chemical order is lower at high temperatures,[18] (2) the free volume may be produced because the free volume decreasing with temperature reaches a equilibrium value, $x_e(T)$, at a temperature T and hereafter increases so as to pursue the $x_e(T)$.[21] The corresponding change is also observed on the $\alpha(300)/\alpha_{as}(300)$ curve. It is noticed that the $\alpha(300)$ becomes more negative as the $\rho(300)$ increases. After about 450 K, $\alpha(300)/\alpha_{as}(300)$ is almost constant. These features of two curves reflect the change in electron transport properties due to the structural relaxation.

To investigate the relaxation behavior at higher temperatures, the isothermal change in $\rho(300)/\rho_{as}(300)$ was measured. Figure 3 shows the resistivity change, $\rho(300)/\rho_{as}(300)$, annealed isothermally at 570 K for as-quenched $Pd_{42.5}Cu_{27.5}Ni_{10}P_{20}$ glass. The $\rho(300)$ reached a

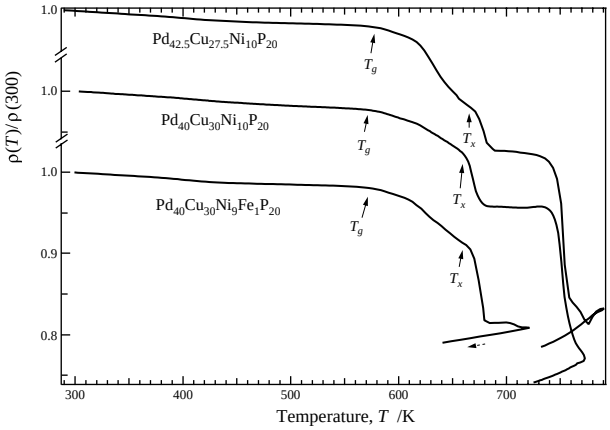

Fig. 1 The electrical resistivity as a function of the temperature for the $Pd_{40}Cu_{30}Ni_{10}P_{20}$, the $Pd_{42.5}Cu_{27.5}Ni_{10}P_{20}$ and the $Pd_{40}Cu_{30}Ni_9Fe_1P_{20}$ glasses, measured at a heating rate of 0.67 K/s under a pure Ar gas flow.

Table 1 Thermodynamic parameters, T_g and T_x, for the $Pd_{40}Cu_{30}Ni_{10}P_{20}$, the $Pd_{42.5}Cu_{27.5}Ni_{10}P_{20}$ glass and $Pd_{40}Cu_{30}Ni_9Fe_1P_{20}$ glasses.

Alloy	T_g	T_x
$Pd_{40}Cu_{30}Ni_{10}P_{20}$	576	662
$Pd_{42.5}Cu_{27.5}Ni_{10}P_{20}$	572	662
$Pd_{40}Cu_{30}Ni_9Fe_1P_{20}$	574	665

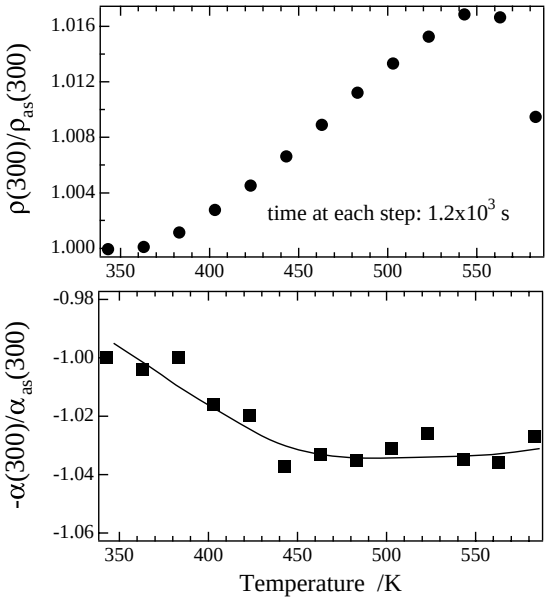

Fig. 2 The Change in the $\rho(300)$ and the $\alpha(300)$ at room temperature for the $Pd_{42.5}Cu_{27.5}Ni_{10}P_{20}$ glass after annealing isochronally for 1.2×10^3 s at a given temperature, where the solid line is drawn as a guide of eyes.

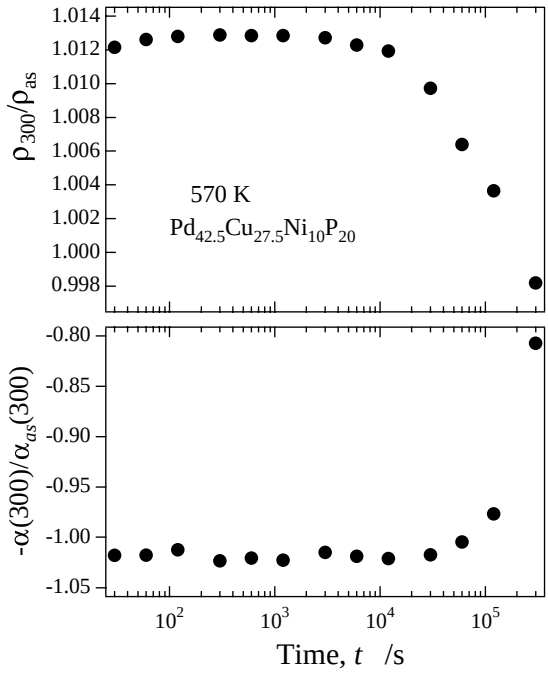

Fig. 3 The change in the $\rho(300)$ and the $\alpha(300)$ after annealing isothermally at 570 K for the $Pd_{42.5}Cu_{27.5}Ni_{10}P_{20}$ glass.

saturation level, approximately 1.2% larger than that of an as-quenched sample, during an initial annealing for 3×10^2 s and remained almost constant up to 6.0×10^3 s. Hereafter, the $\rho(300)$ decreased monotonously up to 3×10^5 s. On the other hand, the $\alpha(300)$ was decreased by about 2.5% after annealing for initial 3.0×10^1 s and remained almost constant up to 3.0×10^4 s. Subsequently, the $\alpha(300)$ increased abruptly. Various reports on the isothermal relaxation process demonstrated that the CSRO process appeared in an initial part of the isothermal annealing curve and the TSRO process followed it.[20,21] At high temperatures nearby T_g, the CSRO process was reported to terminate just after starting

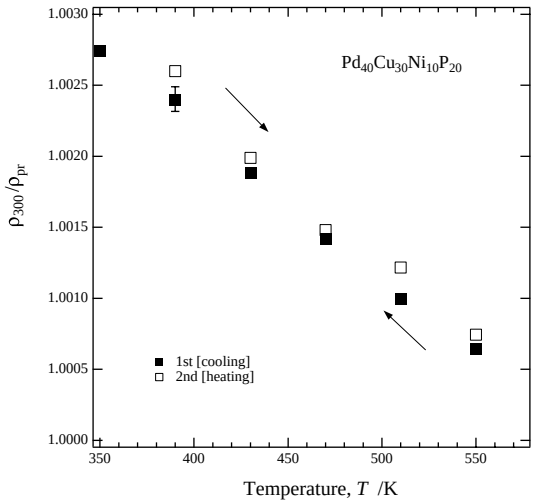

Fig. 4 Isochronal change in the $\rho(300)$ measured between 350 and 550 K. The annealing time was the same as that in Fig. 2. The 1st run was performed from 550 K in a downward direction to room temperature and subsequently the 2nd run was performed up to 550 K.

the heat treatment, typically 10 s on annealing at 575 K for the $Pd_{40}Ni_{40}P_{20}$ glass.[21] Thus the free volume concentration and the degree of the chemical order presumably reached each equilibrium state after annealing for 3×10^2 s. A subsequent monotonous decrease of $\rho(300)$ after annealing for 6×10^3 s corresponds perhaps to a continuous transformation to nanocrystallization and/or amorphous phase separation, because no change except the amorphous halo pattern were detected by X-ray diffraction for the sample annealed for 1.2×10^5 s.

An increase of the resistance observed in an initial stage of curves in Figs. 2 and 3 suggests the existence of CSRO process. To confirm it, we performed the isochronal experiment for the $Pd_{40}Cu_{30}Ni_{10}P_{20}$ glass stabilized by annealing for 6×10^2 s at 600 K in the supercooled liquid region and then cooling down to room temperature at a rate of 0.67 K/s. The change in density was then measured using a water-quenched bulk glass with the weight of approximately 0.3 g. The density of the as-quenched bulk, $9.318 \pm 0.007\,\mathrm{g\,cm^{-3}}$, increased to $9.337 \pm 0.25\,\mathrm{g\,cm^{-3}}$ after stabilizing. The observed density change, about 0.2%, corresponds to the densification due to an elimination of the quenched-in free volume. Figure 4 shows the change of $\rho(300)/\rho_p(300)$ after annealing isochronally for 1.2×10^3 s at each temperature, where $\rho_p(300)$ is the resistivity at 300 K after pre-annealing. During cooling down to room temperature (1st run), the $\rho(300)/\rho_p(300)$ increases and then it decreases again according to subsequent heating procedure (2nd run). Both curves are almost in agreement with each other and this corresponds to the reversible change peculiar to the CSRO process, showing that the formation and the decomposition of a ordered state occurred reversibly over a wide temperature range as predicted from the activation energy spectrum model.[23] It is true in general that the formation of the chemical order is necessary to accompany with the annihilation of the free volume. However, as the present experiment shows, the CSRO process exists actually that does not accompany with an remarkable annihilation of the free volume, although the formation and the decomposition of a chemical order may occur at a site in

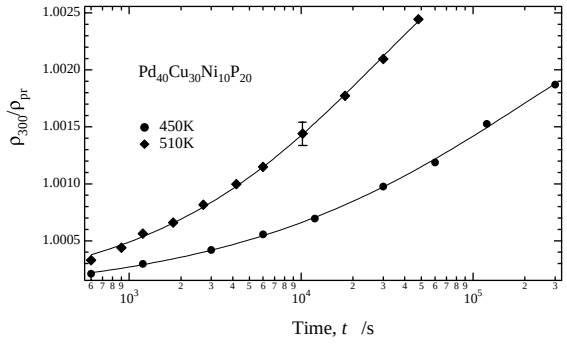

Fig. 5 Isothermal annealing behavior of $\rho(300)$ at 450 (●) and 510 K (◆). Solid lines were obtained by a least square fit using the relaxation function.

the vicinity of a free volume.

To examine the kinetics of the formation of an ordered state, we performed the isothermal experiments. Figure 5 plots the isothermal change in $\rho(300)$ at 450 and 510 K versus the annealing time for stabilized $Pd_{40}Cu_{30}Ni_{10}P_{20}$ glasses. The resistivity increases with time and this demonstrates the extension of a chemical order. Solid lines also represent curves fit by the relaxation function, $\Psi(t) = \frac{\rho(t)-\rho(0)}{\rho_\infty-\rho(0)} = \exp\{-(t/\tau)^n\}$, where τ is the relaxation time. In the present experiment, $n \approx 0.5$ in average was obtained and this gives an evidence for the existence of the activation energy spectrum[10] peculiar to the CSRO process. We conclude that while the formation and the decomposition of the chemical order increases and decreases the resistivity, $\rho(300)$, the release of the quenched-in stress gives rise to an increase of it. In regarding to the free volume, if we assume that the free volume production occurs above about 570 K in the isochronal annealing treatment, the increase and the decrease of the resistivity may correspond to the annihilation and the production of the free volume, respectively. On the other hand, it should be pointed out that the change in $\alpha(300)$ is always opposite in sign to the change in $\rho(300)$.

4. Discussion

4.1 Change in $\rho(300)$ and $(d\rho/dT)_{300}$ due to the change in free volume

In the present experiment, the resistivity $\rho(300)$ increased by the elimination of the free volume and $\alpha(300)$ decreased, on the contrary. We try, here, to give an explanation about the change in $\rho(300)$ and $\alpha(300)$ accompanying with the free volume change. To go further the consideration, the electron transport of the present glasses should be discussed. So, we measured the low temperature electrical resistivity from 4.2 K to room temperature for the $Pd_{40}Cu_{30}Ni_{10}P_{20}$ glass. Figure 6(a) plots the electrical resistivity as a function of the temperature. The change in conductivity, $\Delta\sigma = \sigma(T) - \sigma(0)$, as a function of the temperature was shown also in Fig. 6(b), where $\sigma(0)$ at 0 K was extrapolated from a region proportional to T. The result exhibits that the conductivity varies as $T^{1/2}$ below about 40 K and as T above that temperature, respectively. The $T^{1/2}$ dependence appears again near by room temperature and it continued up to about 430 K (not shown). The similar behavior of the resistivity at low temperatures below room temperature was reported for the Zr–Cu and Zr–Ti–

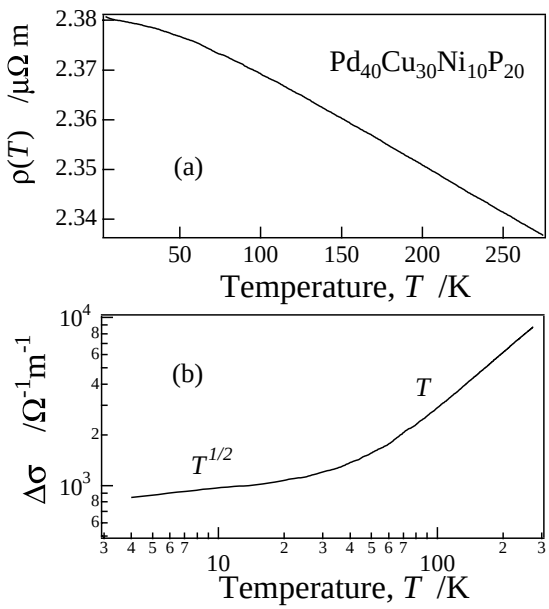

Fig. 6 (a) the low temperature electrical resistivity for the $Pd_{40}Cu_{30}Ni_{10}P_{20}$ glass as a function of the temperature. (b) the temperature dependence of the electrical conductivity change, $\Delta\sigma(T) = \sigma(T) - \sigma(0)$, where $\sigma(0) \approx 4.20 \times 10^6/\Omega$m was obtained by the extrapolation of a T-linear region of $\sigma(T)$ to 0 K.

Be glasses.[24] In this case, the behavior of the conductivity was explained by the weak localization and interaction of conduction electrons. Following this theory, the T-linear region and the $T^{1/2}$ dependence at higher temperatures is due to the localization of conduction electrons. The $T^{1/2}$ dependence of the curve at low temperatures is attributed to the electron-electron correlation effect or the *s-d* interaction effect, and they play so as to destroy the coherence of the electron wavefunction and decrease the resistivity. Within the localization model,[25,26] the temperature independent and dependent parts of the conductivity are given by next equations.

$$\sigma(0) = \sigma_B\left\{1 - \frac{3}{(k_F l_e)^2}\right\}, \quad \sigma_B = \frac{1}{3\pi^2}\left(\frac{e^2}{\hbar}\right)\frac{(k_F l_e)^2}{l_e}, \tag{1}$$

$$\sigma^T(T) = \frac{1}{\pi^2}\left(\frac{e^2}{\hbar}\right)\frac{1}{L_i(T)}, \tag{2}$$

where $L_i^2 = l_e l_i(T)/2$, l_e the mean free length of the electron-ion elastic scattering, l_i the mean free length of the electron-phonon or electron-electron inelastic scattering, and k_F the Fermi wave number. At high temperatures (approximately $T > \Theta/3$, where Θ is the Debye temperature.), l_i^{-1} varies as T and thus $\sigma^T(T)$ varies as $T^{1/2}$. Here, we use the same formulation of l_i as that of the crystal metal and it is represented as below[27]

$$l_i^{-1} = \frac{1}{v_F\tau} = \frac{C^2 m^2 k_B}{\pi c_s^2 d\hbar^4} T, \tag{3}$$

where τ the relaxation time of electron-phonon inelastic scattering, C the deformation potential, d the density of the sample and c_s the sound velocity. The volume and temperature dependent term in eq. (3) is represented as $l_i^{-1} \approx k_F/c_s^2 T$ using the relation, $C \approx E_F$, and the free electron approximation. It is necessary to estimate values, k_F and l_e, to

advance further the discussion. We assumed the relation, $Q_p \approx 2k_F$, used frequently for metallic glasses having a negative TCR, where Q_p is the first peak position of the structure factor. The structure factor of the $Pd_{40}Cu_{30}Ni_{10}P_{20}$ glass was derived from the X-ray diffraction pattern measured with a Mo-$k\alpha$ radiation, and $Q_p \approx 0.291\,nm^{-1}$ was obtained. The $\sigma(0) = 4.19 \times 10^5\,\Omega^{-1}\,m^{-1}$ was obtained by the extrapolation of the T-linear region of the $\sigma(T)$ curve to 0 K. Values k_F and $\sigma(0)$ were substituted into eq. (1) and $l_e \approx 0.290\,nm$ was calculated. The value, $k_F l_e \approx 4.2$, is comparable with those reported for other glasses[24] that the electron transport was well represented by the weak localization model. The changes in $\Delta\rho/\rho_{as}(300)$ and $\Delta\alpha/\alpha_{as}(300)$ due to the free volume reduction were calculated using above equations under the assumption that the free volume reduction causes homogeneously the volume contraction of the sample. The free volume annihilation is expected to cause the volume contraction, $\Delta V/V \approx 3\Delta l/l = -3\beta$ ($\beta > 0$). Then, the corresponding changes are expected to occur in k_F, l_e, and c_s, where we neglect the contribution due to the CSRO process. From a simple consideration, the change, $\Delta\sigma(0) = \sigma(0) - \sigma_{as}(0)$, after the free volume reduction, was given as $\sigma_{as}(0)\beta$, where $\Delta(k_F l_e) \approx 0$ was used. Similarly, the change, $\Delta\sigma^T(300) = \sigma^T(300)(\beta - \Delta c_s/c_s)$, was derived. Therefore, the total change of the conductivity at 300 K, is given as $\Delta\sigma/\sigma_{as} = (\Delta\sigma(0) + \Delta\sigma^T(300))/\sigma_{as} \approx \beta - (\sigma^T(300)/\sigma(0))(\Delta c_s/c_s)$ where we used the relation, $\sigma(0) \gg \sigma^T(300)$. The change in the sound velocity $\Delta c_s^2/c_s^2$ during structural relaxation was measured for the $Pd_{40}Ni_{40}P_{20}$ glass.[22] In this case, by the isothermal annealing at 575 K nearby the T_g, the total change in an as-quenched $c_s^2 = 10.1 \times 10^6\,m^2/s^2$ reached approximately $0.5 \times 10^6\,m^2/s^2$ after an equilibrium was attained. This gives rise to the change, $\Delta c_s/c_s \approx 0.2$. The 30%Cu atoms in the $Pd_{40}Ni_{40}P_{20}$ glass are substituted for Ni ones in the present glass. However, the thermal properties of both glasses are not so different, having the similar glass transition and crystallization temperatures. We believe that the same order of the change, $\Delta c_s/c_s$, as that of the $Pd_{40}Ni_{40}P_{20}$ glass will be observed by the free volume reduction in the Pd–Cu–Ni–P glasses. The ratio, $\sigma^T(300)/\sigma(0) \approx 0.04$, was experimentally estimated from the conductivity curve of the $Pd_{40}Cu_{30}Ni_{10}P_{20}$ glass. Thus, $(\sigma^T(300)/\sigma(0))(\Delta c_s/c_s) \approx 8.0 \times 10^{-3}$ is obtained and this value is larger than $\beta \approx 1.7 \times 10^{-3}$, presumed from the volume change, approximately 0.5%,[16] between an as-quenched and relaxed glasses. This leads to a negative $\Delta\sigma/\sigma_{as} \approx -0.6\%$, *i.e.* an increase of the resistivity. Since an observed $\Delta\sigma/\sigma_{as}$ is approximately -1.0% after reaching a saturation on annealing at 570 K, the calculated result becomes slightly smaller and is perhaps due to an under-estimation of $\Delta\sigma^T(300)$ because of a simplified model for the change, $\Delta l_i(300)$, or no considerations on the CSRO contribution. The free volume production causes the volume dilation, leading to a negative β. Then, the $\Delta c_s/c_s$ is reported to be a negative value.[21] So we may expect a positive $\Delta\sigma/\sigma_{as}$, *i.e.* the decrease of the $\rho(300)$. This explains the decrease of $\rho(300)$ observed in Fig. 2. The similar consideration was applied for $\alpha(300) = (d\rho/dT)_{300}$ (< 0) and the change, $\Delta\alpha(300)/\alpha_{as}(300) \approx -(\beta + \Delta c_s/c_s)$ was derived and it explains qualitatively the reason why the experimental $\Delta\alpha(300)/\alpha_{as}(300)$ is a few times larger than $\Delta\rho/\rho_{as}(300)$ and shows an opposite sign to it.

4.2 Mössbauer spectroscopy for the TSRO process at 570 K

Room temperature Mössbauer measurements were performed for an as-quenched $Pd_{40}Cu_{30}Ni_9Fe_1P_{20}$ glass and one annealed at 570 K for 1.2×10^4 s. Figure 7 shows the Mössbauer spectra for as-quenched and annealed samples, where the horizontal scale is referred to the isomer shift of α-Fe. Each spectrum shows a typical asymmetric doublet peculiar to the metallic glass[28,29] without the magnetic order. Because of a predicted distribution of the electric field gradient at a ^{57}Fe nucleus, the peak width broadens. We decomposed the spectrum by two symmetrical lorenzian doublets. Each half maximum width of the peak is 0.377 and 0.311 mm/s, respectively. These are far larger than a line width, 0.244 mm/s, of two inner lines of a standard α-Fe spectrum and it suggests that the spectrum is comprised of the superposition of various doublets with different field gradients. Thus, it will be best way to calculate a distribution of the quadrupole splitting, *QS*, from Mössbauer spectrum, because *QS* is directly proportional to the component, V_{zz}, of the electric field gradient. However, it is sufficient to use a two-doublets fit for the tentative investigation on the change in the isomer shift and the quadrupole splitting relating to the free volume reduction at 570 K. Figure 8 represents the change in average quadrupole splitting, *QS*, and average isomer shift, *IS*, for individual lorentzian doublet. Both of them decrease by annealing and this feature is in agreement with that of a relaxed $Pd_{40}Ni_{40}P_{20}$ glass.[15] The decrease of *QS* means an improvement of the asymmetrical configuration of atoms around a ^{57}Fe atom and it is perhaps induced by the relaxation of the inner stress due to the annihilation of the free volume, as pointed out by Srolovitz *et al.*[14] The *IS* is proportional to the *s*-electron density at the ^{57}Fe nucleus and is given by the equation,

$$IS = A\left\{|\psi_s^{glass}(0)|^2 - |\psi_s^{\alpha Fe}(0)|^2\right\}, \qquad (4)$$

where the constant, A, contains the change in diameter of the ^{57}Fe nucleus between the ground state and the excited one, and take a negative value. Thus, a decrease of the *IS* is connected with an increase of the *s*-electron density at the ^{57}Fe nucleus. The *IS* of Fe atom was estimated by self-consistent

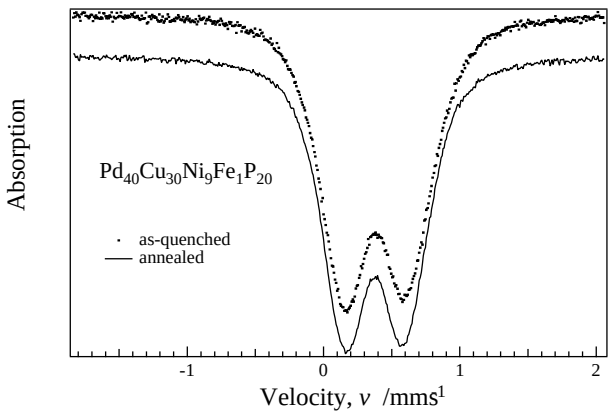

Fig. 7 Mössbauer absorption spectra for as-quenched and annealed (570 K for 1.2×10^4 s) $Pd_{40}Cu_{30}Ni_9Fe_1P_{20}$ glasses.

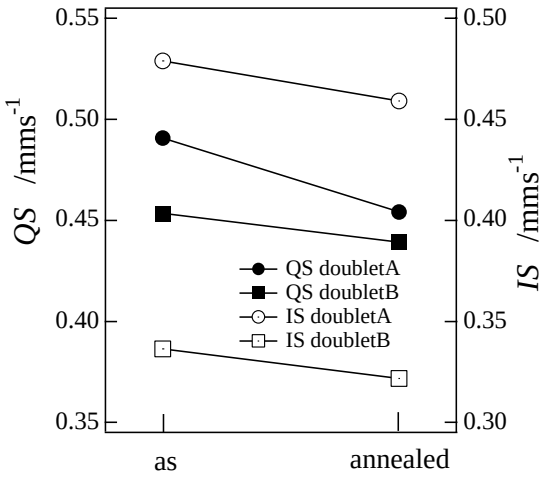

Fig. 8 The change in isomer shift and quadrupole splitting for two decomposed lorentzian doublets (A and B).

calculations[29] for different configurations of the valence electrons. Following this calculation, the *IS* is determined by the valence electron number, $N(=N_s+N_d)$ and N_s, where N_s and N_d are $3s$- and $4d$-electron numbers. The theoretical expression of *IS* is given by the next equation.[28]

$$IS=-1.99-4N_s+0.56N_d+0.36N_s(N_s+N_d). \quad (5)$$

When N is constant, the *IS* decreases linearly with increasing N_s. On the other hand, the *IS* increases with increasing N at constant N_s. The free volume reduction is expected to result in an effective increase of N by the volume contraction. However, under the assumption that a positive change in $\Delta N/N$ was occurred at constant ratio, N_s/N_d, as expected from the volume contraction, an observed average isomer shift, -0.02 mm/s, was difficult to be explained by eq. (5). Thus, a change in ratio, N_s/N_d, should be taken into account to explain the observed isomer shift. But, this is connected with a change in the bonding nature between atoms based on a compositional change around Fe atom and it suggests that an atomic rearrangement, accompanying with a local compositional change, may occur at the annihilation site of the free volume.

5. Summary

The structural relaxation of melt-spun $Pd_{40}Cu_{30}Ni_{10}P_{20}$, $Pd_{42.5}Cu_{27.5}Ni_{10}P_{20}$, glasses was examined by means of the change in the residual resistivity, $\rho(300)$, and the corresponding slope, $\alpha(300)=(d\rho/dT)_{300}$, at room temperature after a given heat treatment. The local change in amorphous structure due to the structural relaxation was investigated by the Mössbauer experiment at room temperature for the $Pd_{40}Cu_{30}Ni_9{}^{57}Fe_1P_{20}$ glass. While the $\rho(300)$ increased with eliminating the quenched-in free volume, the $\alpha(300)$ decreased and showed a few times larger change than that of $\rho(300)$. The existence of the CSRO process was confirmed by the reversible isochronal change in the $\rho(300)$, because there may be few free volume change during annealing due to the stabilization for 6×10^2 s at 600 K in the supercooled liquid region. The formation and the decomposition of a chemical order gave rise to the increase and the decrease of $\rho(300)$, respectively. The change in $\rho(300)$ and $\alpha(300)$ with respect to the elimination of an quenched-in free volume and the production of the free volume to an equilibrium value was understood qualitatively by considerations based on the weak localization model of conduction electrons. The Mössbauer experiments showed the movement of the isomer shift and the quadrupole splitting to a lower position after the sample was annealed to reduce the free volume. Then, it was also suggested that a compositional local change occurred in the vicinity of sites that the free volume disappeared.

REFERENCES

1) N. Nishiyama and A. Inoue: Mater. Trans., JIM **37** (1996) 1531–1539.
2) N. Nishiyama and A. Inoue: Mater. Trans., *in press*.
3) C. Park, M. Saito, Y. Waseda, N. Nishiyama and A. Inoue: Mater. Trans., JIM **40** (1999) 491–497.
4) N. Nishiyama and A. Inoue: Mater. Trans., JIM **40** (1999) 64–71.
5) N. Nishiyama, M. Horino, O. Haruyama and A. Inoue: Appl. Phys. Lett. **76** (2000) 3914–3916.
6) O. Haruyama, H. M. Kimura, N. Nishiyama and A. Inoue: Appl. Phys. Lett. **76** (2000) 2026–2028.
7) A. van den Beukel and J. Sietsma: Acta Metall. Mater. **38** (1990) 383–389.
8) T. Egami: Ann. N.Y. Acad. Sci. **371** (1981) 238.
9) T. Komatsu, K. Iwasaki, S. Sato and K. Matsushita: J. Appl. Phys. **64** (1988) 4853–4859.
10) O. Haruyama: High temperature materials and processes **18** (1999) 1–8.
11) Y. Waseda and T. Egami: J. Mater. Sci. **14** (1979) 1249–1253.
12) Y. Waseda, E. Matsubara, M. Ohzora, A. P. Tsai, A. Inoue and T. Masumoto: J. Mater. Sci. Lett. **7** (1988) 1003–1006.
13) O. Haruyama, K. Sugiyama, S. Kumazawa and Y. Waseda: J. Mater. Sci. Lett. **16** (1997) 1157–1160.
14) D. Srolovitz, T. Egami and V. Vitek: Phys. Rev. B **24** (1981) 6936–6943.
15) R. Brüning, D. H. Ryan and J. O. Ström-Olsen: Hyperfine Interaction **55** (1990) 917–920.
16) N. Nishiyama, M. Horino and A. Inoue: Mater. Trans., JIM. **41** (2000) 1432–1434.
17) H. S. Chen: J. Appl. Phys. **49** (1978) 3289–3291.
18) M. R. J. Gibbs, J. E. Evetts and J. A. Leake: J. Mater. Sci. **18** (1983) 278–288.
19) E. Balanzat, J. T. Stanley, C. Mairy and J. Hillairet: Acta Metall. **33** (1985) 785–796.
20) M. G. Scott and A. Kursumovic: Acta Metall. **30** (1982) 853–860.
21) G. W. Koebrugge, J. Sietsma and A. van den Beukel: Acta Metall. Mater. **40** (1990) 753–760.
22) G. Hygate and M. R. J. Gibbs: J. Phys. F: Met. Phys. **17** (1987) 815–826.
23) M. A. Howson and D. Greig: Phys. Rev. B **30** (1984) 4805–4806.
24) M. A. Howson: J. Phys. F: Met. Phys. **14** (1984) L25–L31.
25) M. Kaveh and N. F. Mott: J. Phys. C: Solid State Phys. **15** (1982) L707–L716.
26) C. Kittle: *Introduction to Solid State Physics*, Seventh edition, (Wiley and Sons, 1996) p. 665.
27) C. Michaelsen, H. A. Wagner and H. C. Freyhardt: J. Phys. F: Met. Phys. **16** (1986) 109–120.
28) C. Michaelsen, M. Meyer and H. C. Freyhardt: J. Appl. Phys. **68** (1990) 269–274.
29) J. L. K. F. de Vries, J. M. Trooster and P. Ros: J. Chem. Phys. **63** (1975) 5256–5262.